Overcoming gain-bandwidth product constraint in slow light Raman amplification with the use of light-stopping schemes

Sunil Sandhu,[1,a)] Michelle L. Povinelli,[2] and Shanhui Fan[1]
[1]*E.L. Ginzton Laboratory, Stanford University, Stanford, California 94305, USA*
[2]*Ming Hsieh Department of Electrical Engineering, University of Southern California, Los Angeles, California 90089, USA*

(Received 7 July 2009; accepted 28 July 2009; published online 25 August 2009)

We show that a light-stopping system with Raman amplification can overcome the gain-bandwidth constraint of slow light Raman amplification systems. The gain scales linearly with the time the pulse spends in the stopped state and is thus much larger than the gain experienced in a slow light system of the same length and operating bandwidth. We present a theoretical analysis of Raman amplification in such a light-stopping system and verify the results using numerical simulations.
 [DOI: 10.1063/1.3211126]

Stimulated Raman scattering (SRS) in Si and GaAs is of recent interest for on chip light amplification.[1–4] Moreover, with the use of slow light waveguides with a large group index n_g,[5–9] it has been shown that signal gain per unit length in the SRS process can be enhanced by a factor of n_g^2,[10] resulting in very compact devices. However, such slow light structures are fundamentally limited by a gain-bandwidth product constraint. As a result, the maximum gain of a slow light structure is inversely proportional to and, hence, is limited by its operating bandwidth. In this letter, we aim to overcome the gain-bandwidth product constraint by considering the Raman amplification process in a light-stopping system consisting of dynamically tuned coupled-resonator delay lines.[11–13] Compared to Raman amplification in a static delay line of the same length, the result is a much larger gain for the same operating bandwidth.

Our Raman amplification system consists of a periodic array of resonators (Fig. 1). Within each unit cell there are two main resonators. Each main resonator has a Raman gain coefficient g and supports both a Stoke mode at a frequency f_s and a pump mode at a frequency f_p, with frequency spacing $f_p - f_s$ corresponding to the optical phonon frequency in the material.[1,2] Such two-mode resonators have previously been designed in photonic-crystal slabs.[14] In the ith unit cell, the Stoke and pump modes in the two resonators have amplitudes $b_i(t)$ and $c_i(t)$ and $p_i(t)$ and $q_i(t)$, respectively. The mode amplitudes are normalized such that the squared amplitude gives the energy in the mode. The coupling rate between neighboring main resonators for the Stoke (pump) mode is $\kappa_s(\kappa_p)$; we assume nearest neighbor coupling only. The chain of main resonators by itself, thus, forms a slow light waveguide[15] that can by itself be used for enhancing Raman effects.

In our system, to allow light stopping, every other main resonator in the system is coupled to a single-mode side resonator with coupling rate κ_s'. The side resonator has mode amplitude $a_i(t)$, with a tunable resonance frequency $f(t)$ in the vicinity of the Stoke frequency. Since such a resonator does not support a resonance at pump frequency, its Raman gain can be ignored.

The system can be described by the following coupled-mode equations, which have been previously shown to accurately describe light propagation in photonic-crystal resonator systems.[11,16]

$$\begin{aligned}
\frac{1}{2\pi}\frac{db_i(t)}{dt} &= jf_s b_i(t) + j\kappa_s[c_{i-1}(t) + c_i(t)] + j\kappa_s' a_i(t) \\
&\quad + g|p_i(t)|^2 b_i(t), \\
\frac{1}{2\pi}\frac{dc_i(t)}{dt} &= jf_s c_i(t) + j\kappa_s[b_i(t) + b_{i+1}(t)] + g|q_i(t)|^2 c_i(t), \\
\frac{1}{2\pi}\frac{da_i(t)}{dt} &= jf(t)a_i(t) + j\kappa_s' b_i(t), \qquad (1) \\
\frac{1}{2\pi}\frac{dp_i(t)}{dt} &= jf_p p_i(t) + j\kappa_p[q_{i-1}(t) + q_i(t)] \\
&\quad - \frac{f_p}{f_s} g|b_i(t)|^2 p_t(t),
\end{aligned}$$

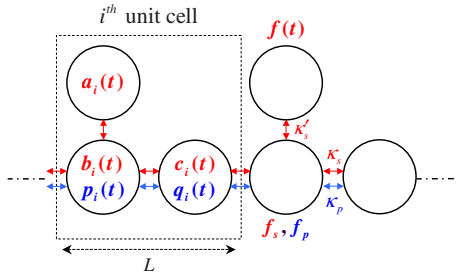

FIG. 1. (Color online) A section of the dynamically tuned coupled-resonator delay line. The unit cell has length L and consists of two main resonators that support both a Stoke mode and a pump mode with resonance frequencies f_s and f_p, respectively, and a single-mode side resonator with dynamic resonance frequency $f(t)$ in the vicinity of the Stoke frequency. $b_i(t)$ and $c_i(t)$ are the modal amplitudes of the Stoke mode, $p_i(t)$ and $q_i(t)$ are the modal amplitudes of the pump mode, and $a_i(t)$ is the modal amplitude of the side resonator. The main resonators have Raman gain coefficient g.

a)Electronic mail: centaur@stanford.edu.

$$\frac{1}{2\pi}\frac{dq_i(t)}{dt} = jf_p q_i(t) + j\kappa_p[p_i(t) + p_{i+1}(t)] - \frac{f_p}{f_s} g|c_i(t)|^2 q_i(t). \quad (2)$$

In the analytic derivation here, we will assume a continuous wave pump with no depletion. Thus, we will set $p_i(t)=q_i(t)=p$ in Eq. (1) and obtain the dispersion equation of the system

$$\cos[kL] = \frac{1}{2\kappa_s^2}[f - f_s + jg|p|^2]\left[f - f_s + jg|p|^2 - \frac{(\kappa_s')^2}{f - f(t)}\right], \quad (3)$$

where k is the Bloch wave vector. The numerical simulations presented below, however, assume the full set of Eqs. (1) and (2) and thus provide a direct check of the approximation regarding no pump depletion.

We simulate the Raman amplification of a signal pulse in the system of Fig. 1 numerically. For concreteness, we choose $f_p - f_s = 15.6$ THz, corresponding to the optical phonon frequency in monolithic silicon,[2] and $f_s = 193.548$ THz, corresponding to a wavelength of 1.55 μm. The side resonator coupling constant is set to $\kappa_s' = 6.19$ GHz. The continuous wave pump copropagates with the input Stoke signal. The pump mode coupling constant $\kappa_p = 31$ GHz was chosen to be larger than the Stoke mode coupling constant κ_s so that the pump mode group velocity will be large relative to the Stoke signal group velocity. This condition was chosen so that the pump energy would not be depleted during the Raman amplification of a Stoke signal pulse. The gain coefficient g is chosen to be $(1.97\times10^{24}/2\pi)$ J^{-1} s^{-1}, as estimated assuming the same resonator design as in Refs. 14 and 16. For a Raman gain $g|p|^2 = 12.5$ MHz, the value of the pump power thus corresponds to an average pump power of 15.5 μW.

In the numerical simulations, the coupled equations [Eqs. (1) and (2)] were solved for a system of $N=315$ unit cells. An additional 35 lossy unit cells were added to the output boundary to absorb the outgoing Stoke and pump signals.

We first consider the case in which the system of Fig. 1 is used as a static delay line. For this purpose, the side cavity is far detuned from the main resonators with a static frequency $f(t) = f_s - 16.65$ GHz. Figure 2(a) shows the system complex frequency [Eq. (3)]. The two upper bands are propagating modes concentrated in the main resonators. Their gain (Im[f]) is close to $g|p|^2$ of the individual resonators.

As a numerical demonstration of the gain-bandwidth product constraint, we simulated the system over a range of system bandwidths ($\kappa_s = 4.86-6.19$ GHz) and Raman gain ($g|p|^2 = 6.25, 12.5, 18.75$ MHz) settings. In each of these simulations, the input Stoke signal used was Gaussian with a center frequency $f_0 \approx f_s$ and a frequency width large enough to occupy a wavevector region of $\Delta k \approx 0.05(2\pi/L)$, around $k \approx 0.4(2\pi/L)$ of the middle band (solid line) in Fig. 2(a), where the dispersion relation is approximately linear. Figure 3(a) shows the amplification of a Stoke signal as it propagates through the structure. Figure 3(b) shows the Stoke signal power gain G performance for different input pulse bandwidths Δf. The gain-bandwidth product $G\kappa_s$ is constant for all values of signal bandwidth Δf.

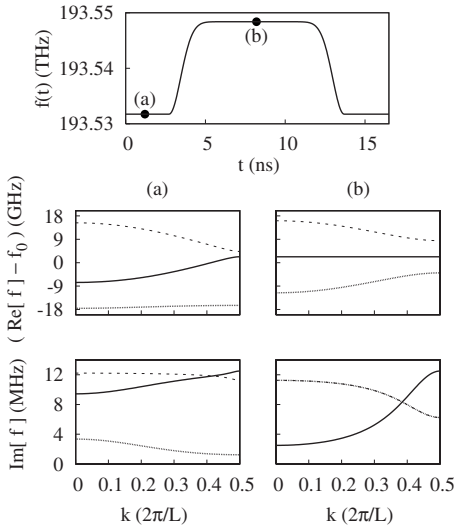

FIG. 2. Topmost plot shows the modulation of the side resonator's resonance frequency (Fig. 1). The bottom set of plots show the band structure of the system at different time instances of the side resonator modulation (as labeled in the modulation plot). Within the bottom set of plots, the top row of plots show the system dispersion Re[f]$-f_0$, while the bottom row of plots show the system gain Im[f]: (a) Initial state $f(t)=f_s-16.65$ GHz. (b) Narrow-bandwidth state $f(t)=f_s$.

We now simulate the Raman amplification process when the system in Fig. 1 operates as a light-stopping system. We again consider the middle band (solid line) of Fig. 2.[11–13] Starting from the large bandwidth state [Fig. 2(a)], as the side resonator is adiabatically tuned toward the main resonator resonance frequency f_s, Re[f] flattens and its frequency bandwidth becomes very narrow when $f(t)=f_s$ [Fig. 2(b)]. In this narrow-bandwidth state, the signal has zero mode amplitude in the main resonators directly coupled to side resonators [i.e., $b_i(t)=0$ in the unit cell of Fig. 1], and the group velocity of the signal is zero.[11–13]

Figure 4(a) shows the time evolution of a Stoke pulse with the same input bandwidth as the slow light example shown in Fig. 3(a). Once the pulse is in the system [Fig.

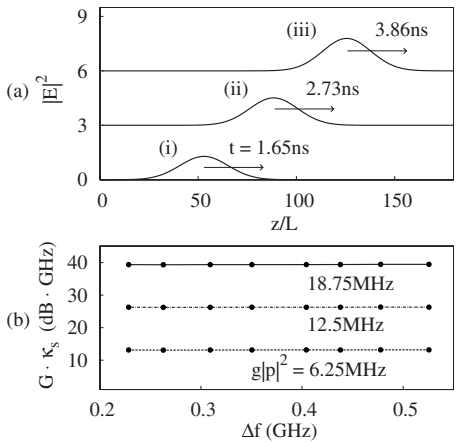

FIG. 3. Static coupled-resonator delay line analysis. (a) Time evolution of Stoke signal with bandwidth $\Delta f = 0.53$ GHz (Raman gain $g|p|^2 = 12.5$ MHz and coupling $\kappa_s = 6.19$ GHz): (i) input pulse, (ii) pulse near the middle of structure, and (iii) output pulse. The power gain over a propagation distance of 218 unit cells was $G = 2.66$ dB. (b) Plot of Stoke signal power gain-bandwidth product $G\kappa_s$ vs Stoke signal bandwidth Δf. For $\Delta f = 0.53$ GHz and $\Delta f = 0.23$ GHz, the system bandwidth κ_s values were 6.19 and 4.86 GHz, respectively.

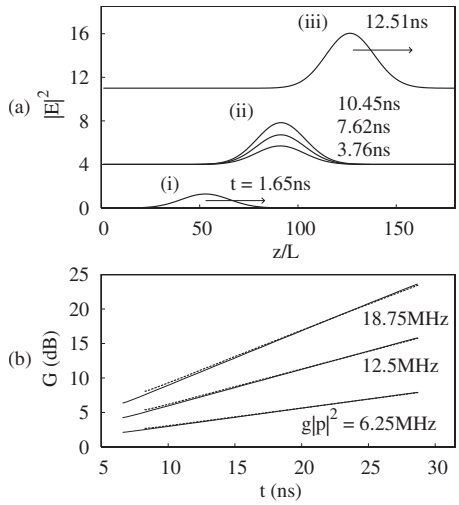

FIG. 4. Dynamically tuned coupled-resonator delay line analysis. (a) Time evolution of Stoke signal with input bandwidth $\Delta f=0.53$ GHz (Raman gain $g|p|^2=12.5$ MHz): (i) input pulse, (ii) different time instances of pulse in narrow-bandwidth stop state, and (iii) output pulse; (b) Stoke signal power gain G over a propagation distance of 218 unit cells versus time delay at different $g|p|^2$ values. For each $g|p|^2$ value, the gain curves for input Stoke signal bandwidths 0.53 GHz (solid line) and 0.23 GHz (dashed line) are shown.

4(a)(i)], $f(t)$ was dynamically tuned from $f_s-16.65$ GHz to f_s, stopping the pulse [Fig. 4(a)(ii)]. [The modulation performed on $f(t)$ corresponds to a refractive index tuning of $\sim 10^{-5}$ which can be achieved by free carrier injection.[17]] In this narrow-bandwidth state, the pulse continues to undergo Raman amplification. After a finite holding time, the dynamic process was applied in reverse to retrieve the signal [Fig. 4(a)(iii)]. Notice that the output pulse is still Gaussian. Figure 4(b) shows the Stoke power gain performance for input pulse bandwidths $\Delta f=0.23$ GHz and $\Delta f=0.53$ GHz. We see that the gain G increases linearly with the holding time of the pulse in the narrow-bandwidth state. In combination with Fig. 3(b), this result thus indicates that the Raman amplification in a light-stopping system is not constrained by the system bandwidth κ_s and can be made much larger than a slow light system of the same length, operating bandwidth and Raman gain $g|p|^2$.

Although the formulation in Eqs. (1) and (2) assumes a lossless system, possible loss mechanisms in the Raman amplification process include radiation loss and two-photon absorption (TPA) induced free-carrier absorption (FCA).[16] One can, in principle, overcome the effect of such loss by increasing the pump power. Moreover, the effects of TPA induced FCA can be reduced by either using a reverse bias structure[18] or by adjusting the pump dynamics.[6,16]

This work was supported in part by the DARPA slow light program under Grant No. FA9550-05-0414.

[1] W. D. Johnston and I. P. Kaminow, Phys. Rev. **188**, 1209 (1969).
[2] J. M. Ralston and R. K. Chang, Phys. Rev. B **2**, 1858 (1970).
[3] R. Claps, D. Dimitropoulos, Y. Han, and B. Jalali, Opt. Express **10**, 1305 (2002).
[4] H. Oda, K. Inoue, N. Ikeda, Y. Sugimoto, and K. Asakawa, Opt. Express **14**, 6659 (2006).
[5] R. Claps, D. Dimitropoulos, V. Raghunathan, Y. Han, and B. Jalali, Opt. Express **11**, 1731 (2003).
[6] A. Liu, H. Rong, M. Paniccia, O. Cohen, and D. Hak, Opt. Express **12**, 4261 (2004).
[7] T. K. Liang and H. K. Tsang, Appl. Phys. Lett. **85**, 3343 (2005).
[8] J. F. McMillan, X. Yang, N. C. Panoiu, R. M. Osgood, and C. W. Wong, Opt. Lett. **31**, 1235 (2006).
[9] H. Oda, K. Inoue, A. Yamanaka, N. Ikeda, Y. Sugimoto, and K. Asakawa, **93**, 051114 (2008).
[10] M. Soljacic and J. D. Joannopoulos, Nature Mater. **3**, 211 (2004).
[11] M. F. Yanik and S. Fan, Phys. Rev. Lett. **92**, 083901 (2004).
[12] M. F. Yanik, W. Suh, Z. Wang, and S. Fan, Phys. Rev. Lett. **93**, 233903 (2004).
[13] S. Sandhu, M. L. Povinelli, M. F. Yanik, and S. Fan, Opt. Lett. **31**, 1985 (2006).
[14] X. Yang and C. W. Wong, Opt. Express **13**, 4723 (2005).
[15] A. Yariv, Y. Xu, R. K. Lee, and A. Scherer, Opt. Lett. **24**, 711 (1999).
[16] X. Yang and C. W. Wong, Opt. Express **15**, 4763 (2007).
[17] M. Lipson, J. Lightwave Technol. **23**, 4222 (2005).
[18] H. Rong, R. Jones, A. Liu, O. Cohen, D. Hak, A. Fang, and M. Paniccia, Nature (London) **433**, 725 (2005).